High Order Reconstruction for Piecewise Smooth Functions

Anne Gelb

Arizona State University

e-mail: ag@math.la.asu.edu, URL: math.la.asu.edu/∼ag.

This work is partially supported by NSF grants CNS 0324957 and DMS 0510813, and by NIH grant EB 02533-01.

Spectral methods for image reconstruction

- Exponential convergence properties for smooth functions.
- Fast computer algorithms (FFT)
- Commonly used in imaging problems: MRI, climatology, seismology, solar imaging, post-processing of numerical partial differential equations.
- Discrete (uniform) data converted to Fourier coefficients.

Spectral methods for image reconstruction

- Underlying function is most often not smooth.
- Occurrence of Gibbs phenomenon.
- Oscillations and reduced order of accuracy.

Gibbs phenomenon

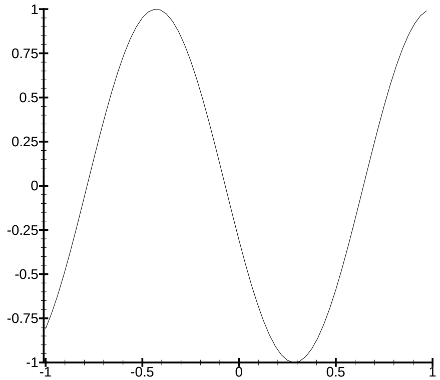

- $f(x) := \cos\left(1.4\pi(x-1)\right)$

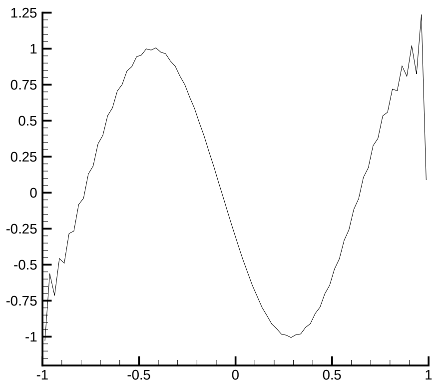

- $S_N[f](x) = \sum_{k=-N}^{N} \hat{f}_k e^{ik\pi x}$

Comments on the Gibbs phenomenon

- $f(x) := \cos(1.4\pi(x-1))$ is piecewise smooth in extension.
- Clearly, there would be no Gibbs phenomenon if an orthogonal polynomial partial sum expansion were used instead, e.g. $S_N[f](x) = \sum_{k=0}^{N} a_k P_k(x)$ where $P_k(x)$ are Legendre or Chebyshev polynomials, but we are given Fourier coefficients.
- There is Gibbs phenomenon for orthogonal polynomial approximation of piecewise smooth functions, for which the following methodology applies (ex: climatology models, co-latitude direction).

Decay rate of Fourier coefficients

- $f(x) \in C^k[-1,1]$ and periodic $\longrightarrow$ very fast decay
- $f(x)$ is piecewise smooth on $[-1,1]$ with M jump discontinuities at

$x = \xi_j, j = 1, \cdots, M$:

$$\begin{aligned} \hat{f}_k &= \frac{1}{2}\int_{-1}^{1} f(x) e^{-ik\pi x} dx \\ &= \sum_{j=1}^{M} [f](\xi_j) \frac{e^{-ik\pi\xi_j}}{2\pi ik} + \frac{1}{2\pi ik}\int_{-1}^{1} f'(x) e^{-ik\pi x} dx \end{aligned}$$

- If $f(x)$ piecewise smooth, the Fourier approximation has spurious oscillations and the convergence rate is first order.

Filtering

- Filtering is standard in medical imaging. It is easy to apply and successfully reduces oscillations and improves the accuracy away from discontinuities.
- Unfortunately, discontinuities get smeared over several grid points, leading to a loss of information of detailed structure. The integrity at the tissue boundaries is compromised, resulting in impaired diagnostic capabilities.

High order image reconstruction

- Two main components

1. **Edge detection:** Develop a method to compute edges of piecewise smooth functions.
2. **Spectral reconstruction in smooth interval:** Develop a method that can restore exponential convergence properties of spectral methods, up to the jump discontinuities.

Edge detection methods

- Edge detection methods are designed to approximate the corresponding jump functions of piecewise smooth functions:
- Global methods (Fourier coefficients):

$$\tilde{S}_N^\sigma f(x) = \sum_{k=-N}^{N} \sigma_k \hat{f}_k e^{ik\pi x} \to [f](x), \quad \text{as } N \to \infty$$

- Local methods (finite differencing):

$$L_m f(x) \to [f](x), \quad \text{with increasingly high order}$$

Concentration method from Fourier data (Gelb and Tadmor)

- Detection of regions of smoothness by “concentrating” at the edges of the piecewise smooth function.
- Application to Fourier coefficients or uniform grid point data in one dimension.
- Simple numerical implementation.
- Fast rate of convergence to zero away from the discontinuities.
- Handles low level of noise.

Concentration method from Fourier data

- Concentration kernel:

$$K_N^\sigma * f(x) = S_N^\sigma[f](x) := i\pi \sum_{k=-N}^{N} sgn(k)\sigma\Big(\frac{|k|}{N}\Big)\hat{f}_k e^{ik\pi x}$$

- Odd kernel: $K_N^\sigma(t) = -\sum_{k=1}^{N} \sigma(\frac{k}{N}) \sin kt$
- Concentration factors $\sigma(\xi)$ satisfy:

1. $\frac{\sigma(\xi)}{\xi} \in C^2[0,1]$
2. $\int_0^1 \frac{\sigma(\xi)}{\xi} d\xi = 1$

- Concentration property

$$K_N^\sigma * f(x) \longrightarrow [f](x) \quad \text{as } N \to \infty.$$

Examples of concentration factors

Concentration factor: $\sigma(q)$, $q = \frac{|k|}{N}$

- Trigonometric factors: $\sigma(q) = \sigma_\alpha(q) := \frac{\sin \alpha q}{Si(\alpha)}$
- Polynomial factors: $\sigma(q) = \sigma^p(q) := pq^p$
- Exponential factors:

$$\sigma(q) = \beta q e^{\frac{1}{\gamma q(q-1)}}, \text{ where } \beta = \int_\epsilon^{1-\epsilon} exp(\frac{-1}{\gamma\eta(\eta-1)}) d\eta$$

Interpretation of concentration factors

- Trigonometric factors:

$$\frac{P_N f(x+\frac{1}{N}) - P_N f(x-\frac{1}{N})}{\frac{2}{\pi}Si(\pi)} \to [f(x)]\delta_\xi(x)$$

- Polynomial factors: Look at higher order derivatives of the spectral projection.

- Exponential factors: Dampen different Fourier coefficients, no physical interpretation.

Polynomial annihilation method (Archibald, Gelb, & Yoon)

- Local method detects regions of smoothness.
- Determines discontinuities in derivatives (subject to constraints).
- Applies to any irregular data in any domain.
- Simple numerical implementation.
- Fast rate of convergence to zero away from the discontinuities.
- The uniform data case can be recast as a concentration kernel for pseudo-spectral Fourier coefficients.

General formulation

- $\mathcal{S}$ is a set of discrete points in the bounded domain $\Omega \subset \mathbb{R}^d$
- f is a piecewise smooth function known only on $\mathcal{S}$
- For any $x \in \Omega$, we choose a set around a point x

$$\mathcal{S}_x := \mathcal{S}_{m_d,x} := \{x_1, \ldots, x_{m_d}\}$$

  where $m_d := \binom{m+d}{d}$
- $L_m f$ for $m \in \mathbb{N}$ is constructed to have the asymptotical convergence property away from jump discontinuities of f:

$$L_m f(x) \longrightarrow 0$$

Local edge detection in two dimensions

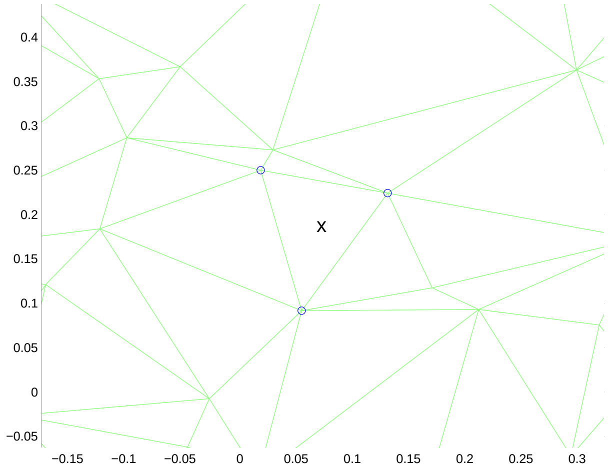

- cell containing possible edge

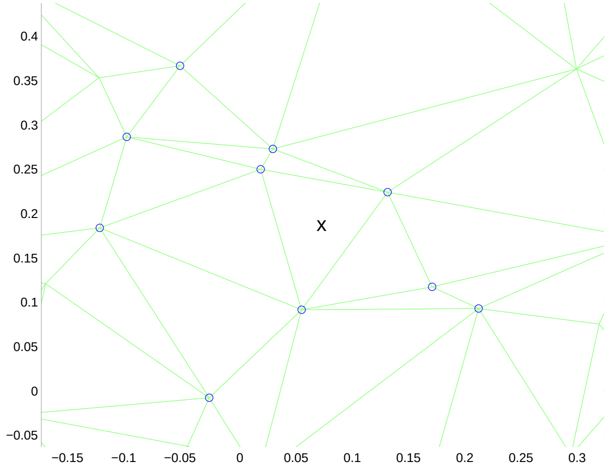

- Set $\mathcal{S}_x$ for given x

Polynomial annihilation property

Solve the linear system

$$\sum_{x_j \in \mathcal{S}_x} c_j(x) p_i(x_j) = \sum_{|\alpha|_1 = m} p_i^{(\alpha)}(x), \quad \alpha \in \mathbb{Z}_+^d,$$

where p_i, $i = 1, \cdots, m_d$, is a basis of Π_m. Here Π_m denotes the space of all polynomials of degree $\leq m$ in $d \in \mathbb{N}$ variables. Note the dimension of Π_m is $m_d := \binom{m+d}{d}$, and therefore the solution exists and is unique.

Edge detection method

The edge detection method computes the approximation of the jump function $[f](x)$

$$L_m f(x) = \frac{1}{q_{m,d}(x)} \sum_{x_j \in \mathcal{S}_x} c_j(x) f(x_j)$$

Here $q_{m,d}(x)$ is a suitable normalization factor depending on m, the dimension d, and the local set $\mathcal{S}_x$.

Example in one dimension

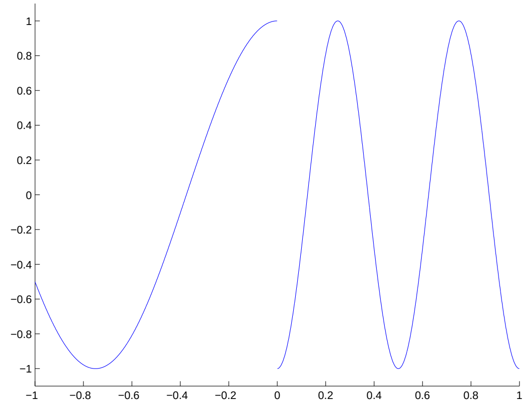

- $f(x) := -\mathrm{sgn}(x) \cdot \cos\left(\frac{4\pi x}{3}(2 + \mathrm{sgn}(x))\right)$

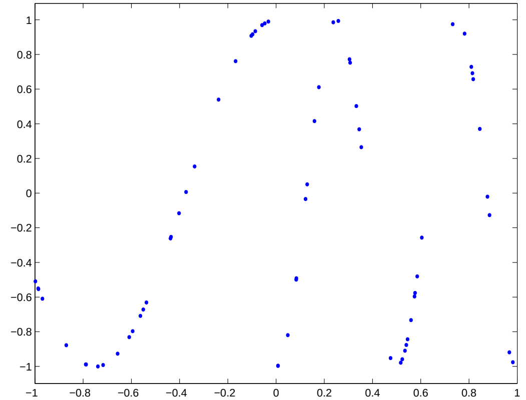

- Random sampling of $f(x)$ on 64 points

Results of local edge detection

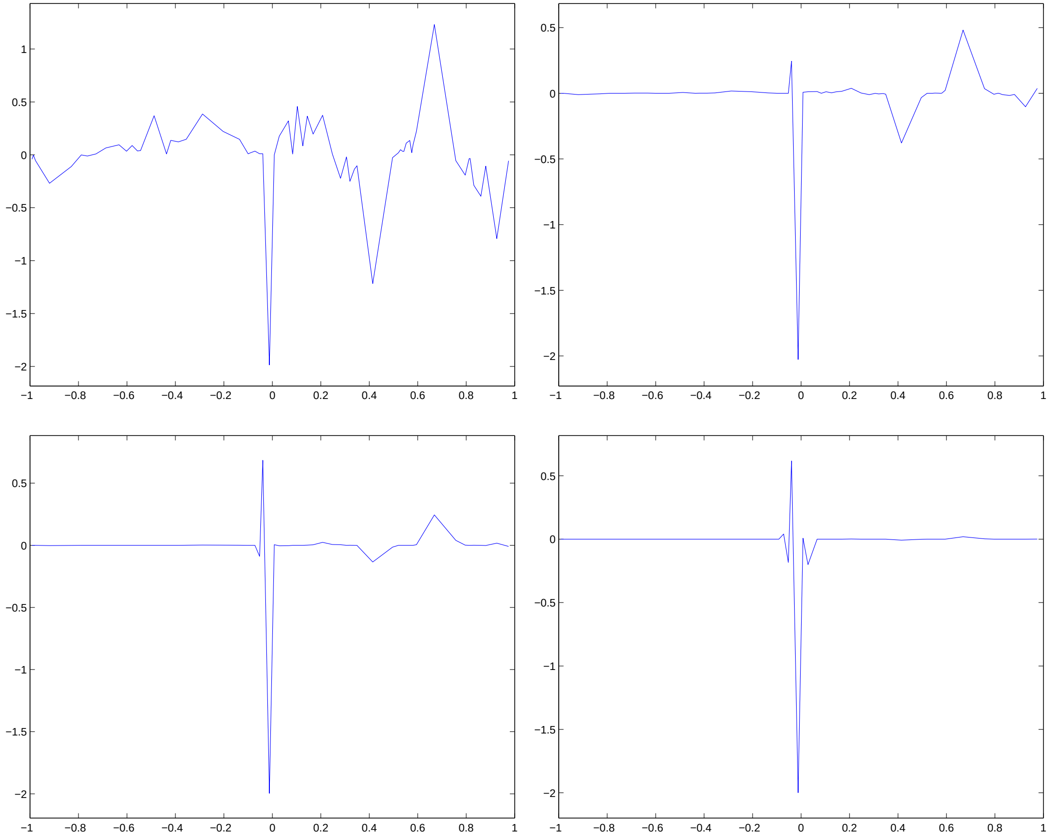

- $L_1 f(x)$
- $L_3 f(x)$
- $L_4 f(x)$
- $L_6 f(x)$

MinMod enhancement of edges

- Define a set of $\mathcal{M}$ (local) edge detectors:

$L_{\mathcal{M}} f = \{L_m f : \mathbb{R} \to \mathbb{R} \,|\, m \in \mathcal{M}\}$.

- Apply the $MinMod$ function:

$$MM\Big(L_{\mathcal{M}} f(x)\Big) = \begin{cases} \min\limits_{m \in \mathcal{M}} L_m f(x), & \text{if } L_m f(x) > 0, \forall m \in \mathcal{M}, \\ \max\limits_{m \in \mathcal{M}} L_m f(x), & \text{if } L_m f(x) < 0, \forall m \in \mathcal{M}, \\ 0, & \text{otherwise.} \end{cases}$$

- Used for both global and local edge detection methods.

- The $MinMod$ relaxes the resolution requirement in any method. Discontinuities can be as close as one pixel apart!

Results of local edge detection using MinMod

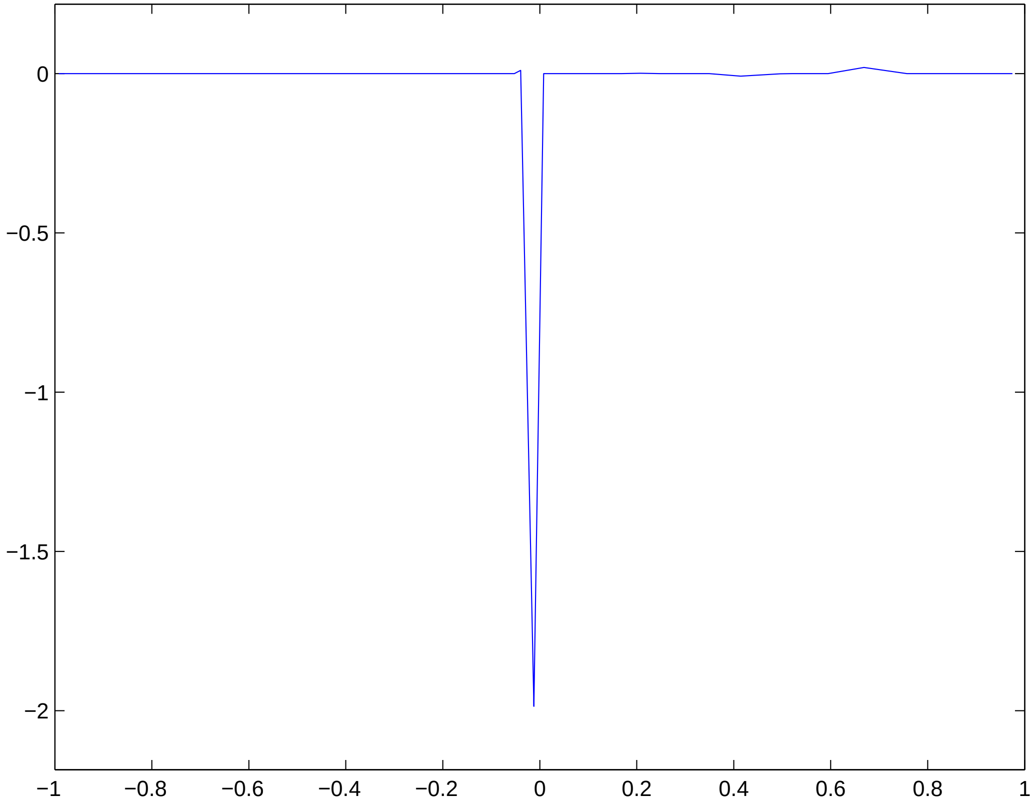

- $MM\left(L_{\mathcal{M}} f(x)\right)$

$\mathcal{M} = \{1, 2, \cdots, 6\}$

Example in two dimensions from medical imaging

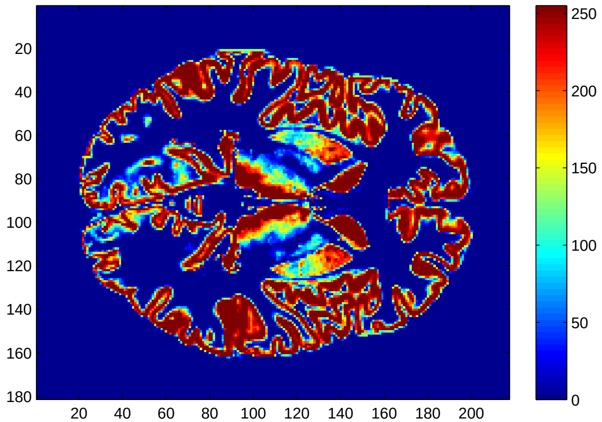

- McConnell Brain (gray matter) from McGill imaging website

18×217 grid

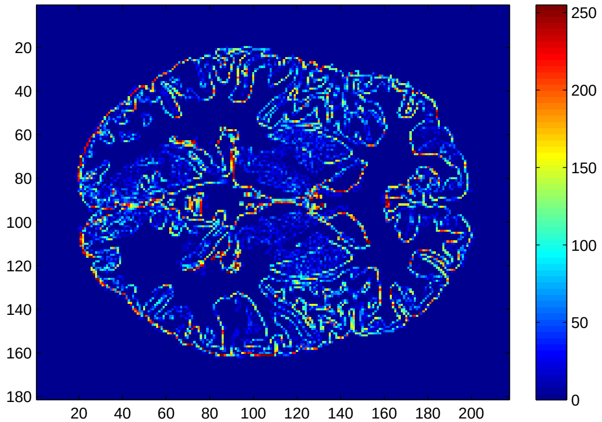

- $MinMod$ application with $\mathcal{M} = \{1,2,3,4\}$.

Spectral reprojection reconstruction method (Gottlieb, Shu)

- Consider a piecewise smooth f on $[-1,1]$ which is analytic but not periodic in a sub-interval $[a,b]$.
- Suppose we are given the Fourier coefficients of this function

$$\hat{f}_k := \frac{1}{2}\int_{-1}^{1} f(y)e^{-ik\pi y}dy, k=-N,\cdots,N.$$

- Linear transformation: $x = \epsilon\xi + \delta$ for $\xi \in [-1,1]$
- Partial sum expansion: $S_N f(x(\xi)) := \sum_{k=-N}^{N} \hat{f}_k e^{ik\pi(\epsilon\xi+\delta)}$
- The spectral method reprojects the original global truncated series approximation onto a new projection basis in smooth subintervals.

Spectral reprojection: Implementation

- $S_N f(x(\xi) := \sum_{k=-N}^{N} \hat{f}_k e^{ik\pi(\epsilon\xi+\delta)}$
- Reproject $S_N f(x(\xi))$ onto a new basis in $[-1,1]$:

$$P_m(S_N f(x(\xi))) := \sum_{l=0}^{m} b_l \psi_l(\xi),$$

where $b_l := \frac{1}{\gamma_l}\int_{-1}^{1} S_N f(x(\xi))\psi_l(\xi)\omega(\xi)d\xi$ and $\psi_l(x)$ are orthogonal with respect to the weight function $\omega(\xi)$, i.e.,

$$(\psi_k(\xi),\psi_l(\xi))_\omega = \int_{-1}^{1} \psi_k(\xi)\psi_l(\xi)\omega(\xi)d\xi = \gamma_l\delta_{kl}$$

Requirements for a reprojection basis (Gottlieb and Shu):

- Definition of a *Gibbs complement*

1. For a function analytic on the interval $[-1, 1]$, the function's expansion in the orthogonal reprojection basis is exponentially convergent.
2. The projection of the high modes in the original basis on the low modes in the new basis is exponentially small.

Convergence of the spectral reprojection method

- Error analysis of the spectral reprojection method:

$$\begin{aligned} Err(m, N, f, \omega) &:= f - P_m(S_N f) = f - P_m f + P_m(f - S_N f) \\ &=: Trunc(m, f, \omega) + Proj(m, N, f, \omega). \end{aligned}$$

- The first component is controlled entirely by the convergence properties of the reprojection basis for m expansion coefficients.
- The second component measures the projection error of the high modes in the original basis onto the low modes in the new basis.

Convergence of the spectral reprojection method

- $Trunc(m, f, \omega) = f - P_m f$

Exponential decay for any orthogonal polynomials satisfying the singular Sturm Liouville equation with m sufficiently large.

- $Proj(m, N, f, \omega) = P_m(I - S_N f)$

$$
\begin{aligned}
P_m(I - S_N f) &= \sum_{l=0}^{m} \psi_l(\xi) \int_{-1}^{1} \omega(\xi)\psi_l(\xi)(f(x(\xi)) - S_N f(x(\xi)))d\xi \\
&= \sum_{l=0}^{m} \sum_{|k|>N} \hat{f}_k \psi_l(\xi) \int_{-1}^{1} e^{i\pi k\xi} \omega(\xi)\psi_l(\xi) d\xi.
\end{aligned}
$$

Choose $\omega(\xi)$ to improve the decay rate of the projection error.

Example of a Reprojection Basis: Gegenbauer polynomials

- The normalized Gegenbauer polynomials: $\psi_l^\lambda(\xi) = \frac{1}{\sqrt{\gamma_l^\lambda}} C_l^\lambda(\xi)$.
- The weighted norm of $C_l^\lambda(\xi)$:

$$\gamma_l^\lambda := \int_{-1}^{1} \omega^\lambda(\xi) C_l^\lambda(\xi) C_l^\lambda(\xi) d\xi = \sqrt{\pi} C_l^\lambda(1) \frac{\Gamma(\lambda + \frac{1}{2})}{\Gamma(\lambda)(l + \lambda)}.$$

- $C_l^\lambda(1) = \Gamma(l + 2\lambda)/l!\Gamma(2\lambda)$.
- Weight function $\omega^\lambda(\xi) = (1 - \xi^2)^{\lambda - \frac{1}{2}}$.
- Orthogonal with respect to the weighted $L^2[-1, 1]$:

$$\int_{-1}^{1} \omega^\lambda(\xi) C_k^\lambda(\xi) C_l^\lambda(\xi) d\xi = 0, \text{ and } k \neq l.$$

Convergence of the Gegenbauer reconstruction method

- weight function $\omega(\xi) = (1-\xi^2)^{\lambda-\frac{1}{2}}, \lambda = \lambda(N)$
- As λ increases, the projection error decays faster:

$$Proj(m, N, f, \omega) = \sum_{l=0}^{m} \sum_{|k|>N} \hat{f}_k \psi_l(\xi) \int_{-1}^{1} e^{i\pi k\xi} \omega(\xi) \psi_l(\xi) d\xi.$$

- As m increases, the truncation error decays faster:

$$Trunc(m, f, \omega) = f - P_m f$$

- Exponential convergence when λ and m both grow with N.

Reconstruction in Magnetic Resonance Imaging (MRI)

MRI reconstruction can be described as the pseudo-spectral Fourier approximation:

$$f_N(x,y) = \sum_{k=-N}^{N} \sum_{l=-N}^{N} \tilde{f}_{k,l} e^{i\pi(kx+ly)}.$$

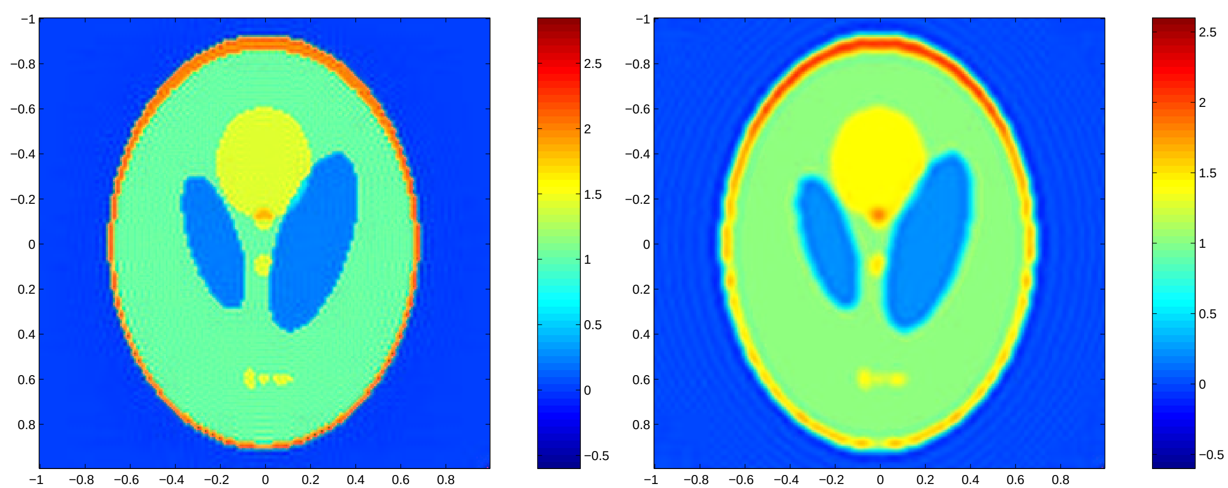

- Shepp Logan
- filtered Shepp Logan

Shepp Logan Gegenbauer reconstruction

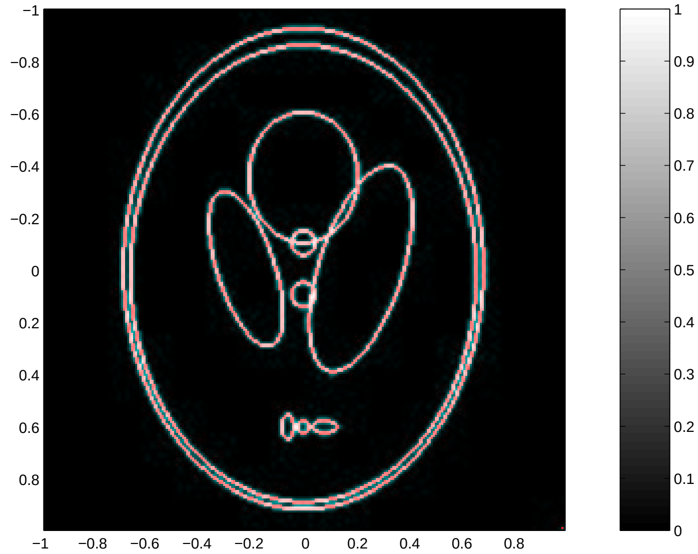

- Edge detection

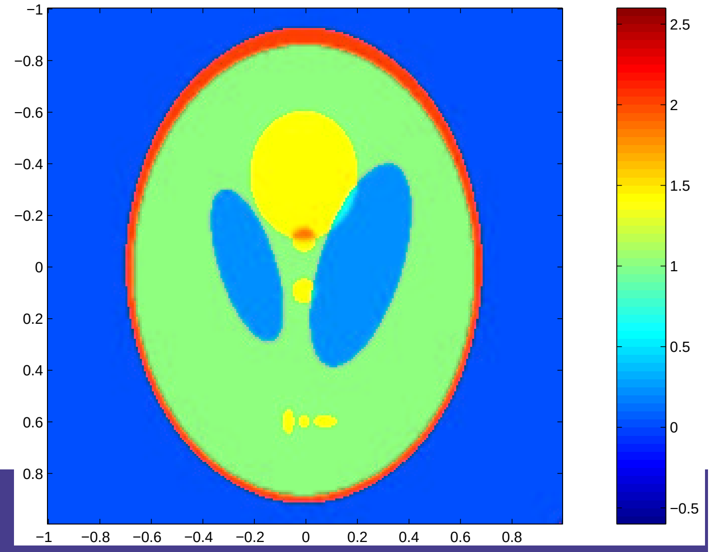

- Gegenbauer reconstruction

Improvement of image quality for segmentation (Archibald, Chen, Gelb, & Renaut)

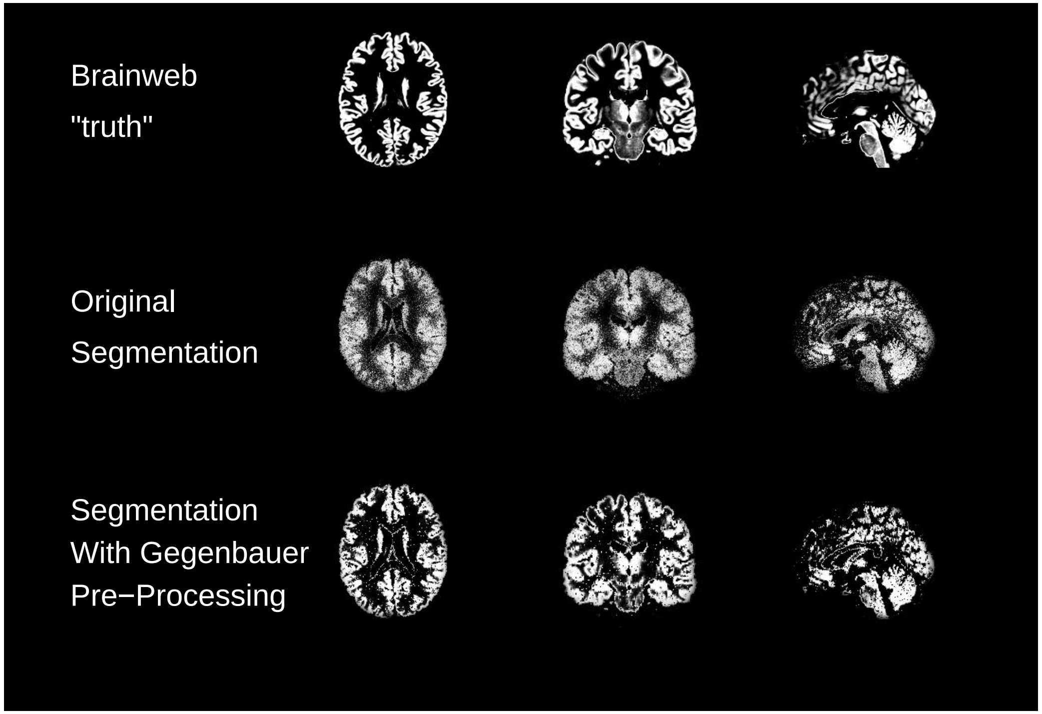

Gray matter segmented probability maps for the original and Gegenbauer image reconstruction of a particular randomly generated MNI digital brain phantom with a 9% level of noise and 40% intensity non-uniformity.

Improvement of image quality for segmentation

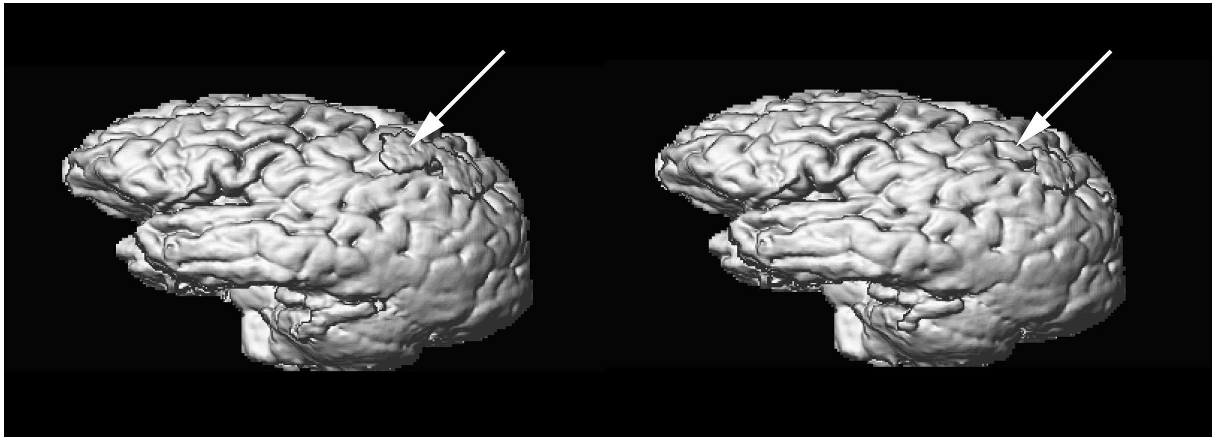 SPM brain extraction of one particular subject, where the picture on the right used edge detection and Gegenbauer reconstruction as a pre-segmentation step.

Mouse brain study

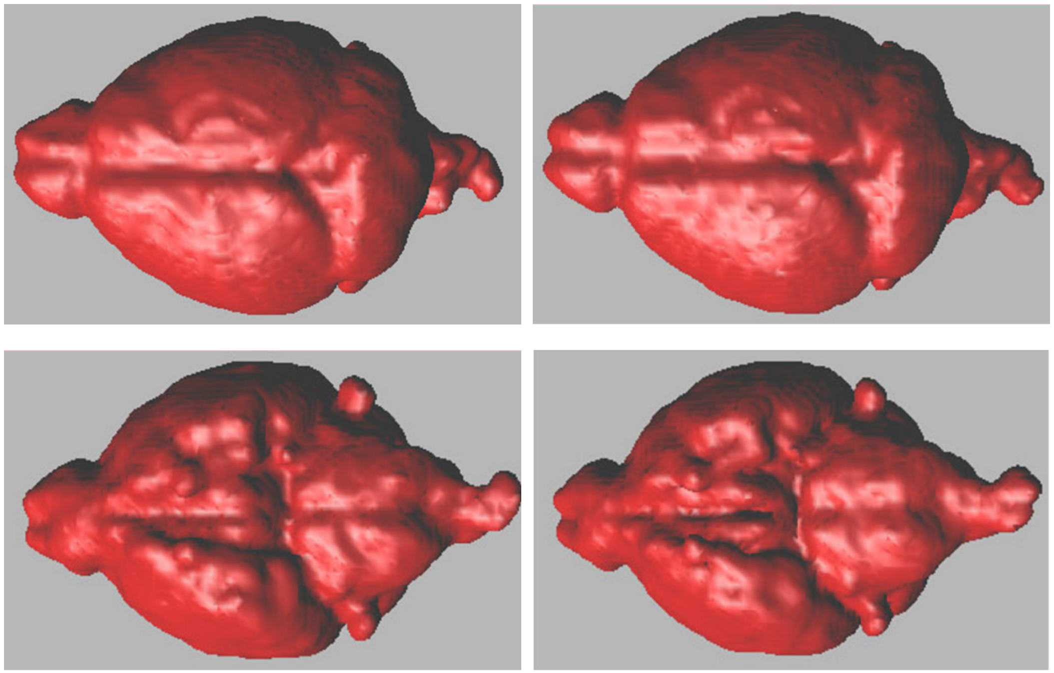

- Top view of mouse brain
- Gegenbauer reconstruction

- Bottom view of mouse brain
- Gegenbauer reconstruction

Concluding remarks and Future Work

- Robustness with respect to noise.
- Other spectral projections besides Fourier can also be used.
- FFT can still be used when Fourier coefficients are original projection.
- Improvement of all segmentation after Gegenbauer pre-processing.
- Ideal for MRI because of Radon and Fourier transform relationship.
- Parameters for MRI do not need much tuning.
- Less misdiagnosis since boundary integrity not compromised.
- Great for low resolution environments.
- Achieve high order reconstruction from other polynomial bases
- Applications to compression.

Some references

- R. Archibald and A. Gelb, A method to reduce the Gibbs ringing artifact in MRI scans while keeping tissue boundary integrity, IEEE Trans. Medical Imaging, 21(2002), 305–319.
- R. Archibald and A. Gelb, Reducing the effects of noise in image reconstruction, J. Sci. Comput., 17(2002), 167–180.
- R. Archibald, K. Chen, A. Gelb and R. Renaut, Improving Tissue Segmentation of Human Brain MRI Through Pre-Processing by the Gegenbauer Reconstruction Method, NeuroImage, 20(2003), 489–502.
- R. Archibald, J. Hu, A. Gelb and G. Farin, Improving the Accuracy of Volumetric Segmentation Using Pre-Processing Boundary Detection and Image Reconstruction, IEEE Transactions on Image Processing, 13(2004), 459–466.
- R. Archibald, A. Gelb, and J. Yoon, Polynomial Fitting for Edge Detection in Irregularly Sampled Signals and Images, Accepted to SIAM J. Numer. Anal., August, 30, 2004.
- J.P. Boyd, Trouble with Gegenbauer Reconstruction for Defeating Gibbs' Phenomenon: Runge Phenomenon in the Diagonal Limit of Gegenbauer Polynomial Approximations, J. of Comp. Phys., in press, (2005).

Some references

- G. FREUD, Orthogonal Polynomials, Pergamon press, Oxford, 1971.
- W. GAUTSCHI, Orthogonal Polynomials: Computation and Approximation, Numerical Mathematics and Scientific Computation Series, Oxford University Press, 2004.
- A. GELB AND E. TADMOR, Detection of edges in spectral data II. Nonlinear enhancement, SIAM J. Numer. Anal. 38(2000), 1389–1408.
- A. GELB AND E. TADMOR, Spectral reconstruction of piecewise smooth functions from their discrete data, M2AN Math. Model. Numer. Anal. 36(2002), 155–175.
- A. GELB AND J. TANNER, Robust reprojection methods for the resolution of the Gibbs phenomenon, to appear in ACHA, 2005.
- D. GOTTLIEB AND C.W. SHU, On the Gibbs phenomenon and its resolution, SIAM Rev. 39(1997), 644–668.
- D. GOTTLIEB AND C.W. SHU, A general theory for the resolution of the Gibbs phenomenon, Atti dei Convegni Lincei 147(1998), 39–48.

Some references

- J.H. JUNG AND B.D. SHIZGAL, Generalization of the inverse polynomial reconstruction method in the resolution of the Gibbs phenomenon, J. Comp. Appl. Math. 172(2004), 131–151.
- Z. P. LIANG AND P. LAUTERBUR, *Principles of Magnetic Resonance Imaging*, IEEE Press (2000).
- MONTREAL NEUROLOGICAL INSTITUTE http://www.mni.mcgill.ca.
- A.F. NIKIFOROV, S.K. SUSLOV, V.B. UVAROV, Classical Orthogonal Polynomials of a Discrete Variable, Springer-Verlag, 1991.